Calculation and Analysis of the Rejected Takeoff Speed of a Commercial Airliner under various Environmental Conditions

James Gonzalez* and Thomas Lombaerts†
San José State University, San Jose, CA, 95121, Santa Clara County

The rejected takeoff (RTO) speed of a commercial airliner is a pivotal parameter that is determined prior to departure to reduce the likelihood of catastrophic runway excursions in the event of an aborted takeoff. Moreover, the ramifications can be disastrous and fatal if the takeoff procedure is aborted after the RTO speed is exceeded, as runway excursions are likely to occur. As a result, the calculation of the RTO speed should be as accurate as possible so that flight crews can make the appropriate decisions during the takeoff procedure. In addition to aircraft specifications and intensive thermodynamic properties, environmental factors such as headwinds, tailwinds, and runway surface conditions impact the RTO speed. The primary objective of the present work is to analyze the effects of wind speed and unfavorable runway conditions on the RTO speed of an Airbus A380-800 with 1-D equations of motion. Realistic wind conditions are collected from METAR observations and unfavorable runway friction coefficients are obtained from existing literature. Through a 2-D sensitivity analysis, the results in the present work show that headwinds coupled with favorable, dry runway conditions increase the magnitude of the RTO speed and prolong the RTO threshold along the runway.

I. Nomenclature

AR	=	Aspect Ratio [-]
b	=	Wingspan [m]
$C_{D_0,L}$	=	Parasitic drag coefficient with spoilers deployed [-]
$C_{D_0,TO}$	=	Parasitic drag coefficient in the takeoff configuration [-]
$C_{D,L}$	=	Total drag coefficient in the landing configuration [-]
$C_{D,TO}$	=	Total drag coefficient in the takeoff configuration [-]
$C_{L,L}$	=	Maximum lift coefficient in the landing configuration [-]
$C_{L,TO}$	=	Maximum lift coefficient in the takeoff configuration [-]
D_L	=	Drag force in the landing configuration [N]
D_{TO}	=	Drag force in the takeoff configuration [N]
dt	=	Timestep [s]
e_1	=	Span efficiency factor [-]
$F_{\text{eff,L}}$	=	Effective force in the landing configuration [N]
$F_{\text{eff,TO}}$	=	Effective force in the takeoff configuration [N]
$\vec{F}_{\text{net}}$	=	Sum of the forces on the aircraft [N]
g_0	=	Acceleration constant due to gravity evaluated at sea-level [$^m/_{s^2}$]
h	=	Height of wingtip above the ground [m]
H_{g}	=	Elevation of the airport above sea-level [m]
L_L	=	Lifting force in the landing configuration [N]
L_{TO}	=	Lifting force in the takeoff configuration [N]
m_{MTOW}	=	Mass of aircraft at MTOW [kg]
ϕ	=	Ground effect factor [-]
ρ_0	=	Density of air evaluated at sea-level [$^{kg}/_{m^3}$]
R	=	Resistance force [N]

*Graduate Student, Department of Aerospace Engineering, Student Member 1217326
†Adjunct Professor, Aerospace Engineering Department, Charles W. Davidson College of Engineering. Aerospace Research Engineer, KBR, Intelligent Systems Division, Mail Stop 269-1, AIAA Associate Fellow, email: thomas.lombaerts@nasa.gov

S = Total wing surface area [m^2]
$S_{L,\text{pub}}$ = Published landing distance [m]
$S_{TO,\text{pub}}$ = Published takeoff distance [m]
S_1 = Location of the rejected takeoff speed [m]
$S_{28\text{R}}$ = Length of runway 28R at KSFO [m]
T_{max} = Maximum thrust [N]
T_{rev} = Reverse thrust [N]
$\mu_{\text{r,L}}$ = Runway friction coefficient in the landing configuration for a dry runway [-]
$\mu_{\text{r,TO}}$ = Runway friction coefficient in the takeoff configuration for a dry runway [-]
$\mu_{\text{r}_{\text{wet}},\text{L}}$ = Runway friction coefficient in the landing configuration for a wet runway [-]
$\mu_{\text{r}_{\text{wet}},\text{TO}}$ = Runway friction coefficient in the takeoff configuration for a wet runway [-]
V = Airspeed [$^m/_s$]
V_1 = Rejected takeoff speed [$^m/_s$]
$V_{L,\text{pub}}$ = Published landing speed [$^m/_s$]
$V_{TO,\text{pub}}$ = High-end of published takeoff speed [$^m/_s$]
V_{wind} = Wind speed [$^m/_s$]
W_f = Weight of aircraft fuel [N]
W_{MTOW} = Maximum takeoff weight [N]
W_{ZFW} = Zero fuel weight [N]
$\ddot{x}\,(t)$ = Instantaneous inertial acceleration [$^m/_{s^2}$]
$\dot{x}\,(t)$ = Instantaneous ground speed [$^m/_s$]
$x\,(t)$ = Instantaneous position [m]

II. Introduction

The rejected takeoff (RTO) speed, commonly referred to as V_1, is the maximum speed by which a rejected takeoff must be initiated to ensure an aircraft does not overshoot the runway [1]. Moreover, the RTO speed of a commercial airliner carrying passengers, cargo, and fuel is a vital parameter that is calculated prior to departure to reduce the likelihood of catastrophic runway excursions in the event of an emergency during the takeoff procedure (e.g., compressor stalls due to bird strikes, blown tires, runway incursions by other aircraft, etc.). Baseline V_1 calculations incorporate several factors such as aircraft performance and geometry (e.g., takeoff thrust, aspect ratio, etc.), airport information (e.g., runway length, field elevation, etc.), and intensive thermodynamic properties (e.g., air density, ambient temperature, etc.) [2]. However, environmental factors such as headwinds, tailwinds, and unfavorable runway surface conditions impact the V_1 calculation as well as the overall performance of the aircraft during the ground roll [3, 4]. Therefore, environmental factors are included in the V_1 calculation so that flight crews can make the appropriate go/no-go decision during the takeoff procedure.

The RTO speed of a commercial airliner under various environmental conditions is investigated through a 2-D sensitivity analysis in the present work. First, the problem statement, coordinate system, free body diagrams (FBD), and assumptions are defined in Sect. 3. Next, the calculated baseline RTO speed is presented and validated with published data in Sect. 4. Following the baseline model, the effects of headwinds, tailwinds, and various runway surface conditions on the RTO speed are presented in Sect. 5. Lastly, a comprehensive summary of the present work as well as future tasks are presented in Sect. 6.

III. Problem Description and the Aircraft Model

Considered the world's largest civilian passenger jet in history, the four-engine Airbus A380-800 at maximum takeoff weight (MTOW) is the commercial airliner selected for this study [5]. Furthermore, the airport and runway selected for this study are San Francisco International Airport (KSFO) and runway 10L/28R, respectively. Of the four runways at KSFO, 10L/28R is the longest and is the most appropriate option for an A380 at MTOW [6]. Moreover, the A380 is setup for a west departure based on average wind conditions obtained from METAR observations [7].

The primary objective of the present work is to analyze the effects of headwinds, tailwinds, and wet runway conditions on the RTO speed of an A380 with 1-D equations of motion. Prior to the implementation of environmental factors, a baseline model is constructed given readily accessible, published A380 data and specifications such as MTOW, wing geometry, and the height of the wingtip above the ground [5, 8]. Moreover, KSFO information such as

runway length are included in the baseline model. The baseline case assumes negligible wind speeds and regular, dry runway conditions. In addition, the baseline model is validated with published, nominal A380 takeoff and landing data [8]. Given a proven model, realistic wind conditions obtained from METAR observations as well as approximated expressions for wet runway friction coefficients are implemented to assess environmental impacts on V_1 [7, 9].

A. Free Body Diagrams

The 1-D governing equation of motion used in the present work is Newton's second law as shown in Eq. (1) below. Moreover, the positive convention in the present work is in the same direction as the ground speed $\dot{x}$. The calculation of the RTO speed in this study is determined based on the intersection point between the takeoff and landing velocity profiles during the ground roll. Moreover, the velocity profiles are obtained by integrating the instantaneous acceleration $\ddot{x}\,(t)$ in Eq. (1), which is dependent on the effective forces.

$$\Sigma \vec{F}_{\text{net}} = m_{MTOW}\ddot{x}\,(t) \tag{1}$$

For the baseline study, the effective forces acting on the aircraft are thrust, drag, lift, weight, and friction resistance between the runway and the landing gear wheels as shown in Fig. 1(a) below. Furthermore, the configuration and arrangement of the force vectors in the baseline takeoff FBD (refer to the top schematic in Fig. 1(a) below) agree with existing literature [2]. In the baseline landing FBD (refer to the bottom schematic in Fig. 1(a)), reverse thrust is engaged to decelerate the A380 in the event of a RTO. Additionally, the lifting force in the baseline landing FBD is omitted because the spoilers along the wing are engaged. Furthermore, the smaller $\dot{x}$ vector in the baseline landing FBD indicates the aircraft is decelerating.

The FBD for the environmental factor study include the same effective forces as the baseline study with the addition of a wind speed component, as shown in Fig. 1(b) below. Moreover, headwinds as depicted in Fig. 1(b) increase the airspeed of an aircraft as well as the magnitude of the aerodynamic forces (e.g., lift and drag). On the other hand, tailwinds slow down the airflow over the wing which ultimately reduces the aerodynamic forces during the takeoff procedure.

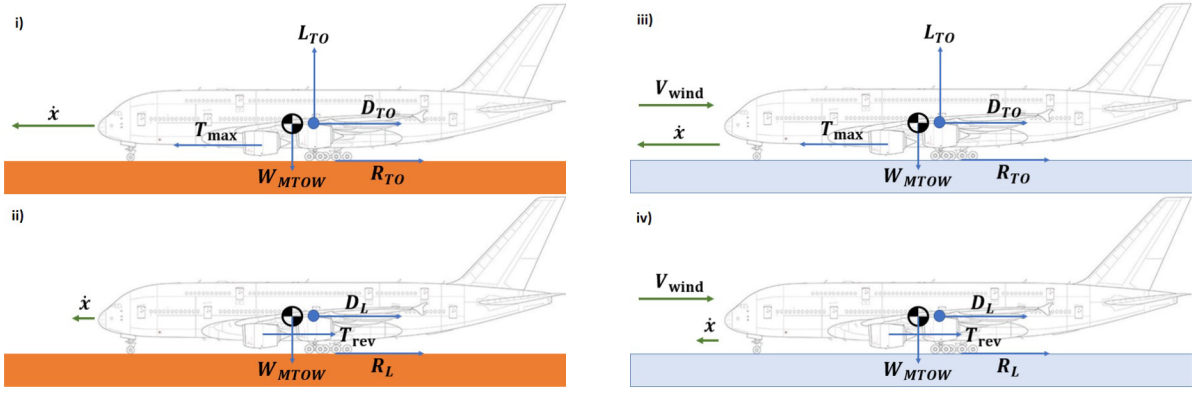

(a) Baseline (b) Environmental factors

Fig. 1 Free body diagrams and effective forces acting on the aircraft

B. Assumptions

For simplification purposes, several assumptions are implemented in the present work. Regarding the airfield, the runway slope is omitted because the difference in elevation between the runway ends, 28R and 10L, is negligible [6]. Furthermore, the runway is assumed to be paved and smooth and average, dry runway coefficients are easily obtainable from existing literature [2]. Regarding the aircraft, the weight is assumed to remain constant since the present work is focused specifically on the ground roll. During the takeoff procedure, the thrust force is directly in-line with the engines and the thrust inclination angle is negligible. With the spoilers engaged in the landing configuration, it is assumed all of the lift is disturbed based on the spoiler coverage along the wing [8]. Since the model specifically captures the ground

roll, moments about the center of mass and the aerodynamic center are not considered in the analysis. Due to the limited information on the planform geometry, a span efficiency factor, e_1, of 0.90 is assumed. Moreover, the value selected for e_1 lies within an acceptable range for typical subsonic aircraft [2]. Regarding the effective force calculations, the lift generated by the fuselage and horizontal stabilizer is neglected. For the ground effect calculation, the A380 winglet design is neglected for simplification purposes. For the environmental factors described in the present work, the runway friction coefficients are averaged and remain constant throughout the ground roll and pure headwinds and tailwinds are assumed.

IV. Baseline Study and Model Development

Specifications and characteristics of the A380 are obtained from readily available fact sheets and maintenance manuals, and are presented in Table 1 below [5, 8]. The published landing velocity of the A380, $V_{L,\text{pub}}$, is the indicated airspeed with certified maximum flap setting and standard atmospheric conditions [8]. The published takeoff distance of the A380 $S_{TO,\text{pub}}$ used for this analysis assumes zero pressure altitude based on the airport elevation, International Standard Atmosphere (ISA) conditions, and negligible wind factors [8]. In addition, the published landing distance $S_{L,\text{pub}}$ is based on dry runway conditions as well as field elevation [8].

Table 1 Published data for Airbus A380-800 at sea-level [5, 8]

Parameter	Value	Units
b	79.75	m
S	845	m^2
AR	7.53	–
h	7.8	m
$V_{TO,\text{pub}}$	87.5	m/s
$V_{L,\text{pub}}$	71.0	m/s
$S_{TO,\text{pub}}$	3,000	m
$S_{L,\text{pub}}$	2,150	m
m_{MTOW}	575,000	kg
W_{MTOW}	5,638,800	N
W_f	2,490,700	N

Information related to KSFO is obtained from readily accessible published data, and is noted in Table 2 below [6]. Moreover, the density and the acceleration due to gravity are evaluated at sea-level since the airport elevation H_g is negligible compared to the radius of Earth [2].

Table 2 KSFO airport information [6]

Parameter	Value	Units
$S_{28\text{R}}$	3,618	m
H_g	4.10	m
ρ_0	1.225	kg/m^3
g_0	9.81	m/s^2

The aerodynamic properties for both the takeoff and landing configurations are calculated with published aircraft and airport data noted in Table 1 and Table 2. Moreover, the aerodynamic properties assume steady, level flight conditions where the weight of the aircraft is equivalent to the lifting force. The coefficient of lift for the takeoff procedure, $C_{L,TO}$, incorporates MTOW conditions as well as the A380 published takeoff speed as shown in Eq. (2) on the following page. Similarly, the coefficient of lift for the landing procedure, $C_{L,L}$, incorporates the weight of the aircraft without fuel

W_{ZFW} (refer to Eq. (3) below) and the published landing speed as shown in Eq. (4) below. Moreover, the flap settings for the takeoff and landing configurations are captured in $V_{TO,\text{pub}}$ and $V_{L,\text{pub}}$, respectively.

$$C_{L,TO} = \frac{W_{MTOW}}{\frac{1}{2}\rho_0 V_{TO,\text{pub}}^2 S} \tag{2}$$

$$W_{ZFW} = W_{MTOW} - W_f \tag{3}$$

$$C_{L,L} = \frac{W_{ZFW}}{\frac{1}{2}\rho_0 V_{L,\text{pub}}^2 S} \tag{4}$$

Since the present work is focused specifically on the ground roll, the approximated ground effect factor, ϕ, is obtained with Eq. (5) [2]. The approximated ground effect factor is included in the analysis to diminish the strength of the wing-tip vortices due to the interaction with the runway surface [2]. Moreover, the disturbance of the wing-tip vertices ultimately reduces the induced drag and the overall drag penalty. The approximated downwash for this study was calculated to be $\phi = 0.71$.

$$\phi = \frac{\left(\frac{16h}{b}\right)^2}{1 + \left(\frac{16h}{b}\right)^2} \tag{5}$$

The total drag coefficient for the takeoff configuration, $C_{D,TO}$, includes both the parasitic and induced drag components and is obtained with Eq. (6). Moreover, a span efficiency factor of $e_1 = 0.90$ is selected for this study since the value lies halfway between the acceptable range for typical subsonic aircraft [2]. In addition, the induced drag component of Eq. (6) is reduced by ϕ since it is less than unity. The total drag coefficient for the landing configuration $C_{D,L}$ only includes the parasitic drag component as shown in Eq. (7) since the spoilers are engaged and all of the lift over the wing is disturbed. Moreover, the parasitic drag components for Eq. (6) and Eq. (7) were approximated with Breguet's equations [2]. All of the required dimensionless aerodynamic properties for the present work are included in Table 3 below.

$$C_{D,TO} = C_{D_0,TO} + \phi \frac{C_{L,TO}^2}{\pi e_1 AR} \tag{6}$$

$$C_{D,L} = C_{D_0,L} \tag{7}$$

Table 3 Approximated Airbus A380-800 aerodynamic properties

Parameter	Value
$C_{L,TO}$	1.4245
$C_{L,L}$	1.2069
$C_{D_0,TO}$	0.0130
$C_{D_0,L}$	0.0143

The forces acting on the aircraft for the takeoff and landing baseline case are obtained from the FBD (refer to Fig. 1(a) on pg. 3). Given $C_{L,TO}$ and $C_{L,L}$, the lifting forces for the takeoff and landing configurations are obtained with Eq. (8) and Eq. (9), respectively. Similarly, given $C_{D,TO}$ and $C_{D,L}$, the drag forces for the takeoff and landing configurations are obtained with Eq. (10) and Eq. (11), respectively. For the present work, the maximum takeoff thrust is set to $T_{\text{max}} = 979,968\ N$ and the reverse thrust T_{rev} is approximated at 15% of T_{max}. Regarding the baseline runway conditions, the dimensionless runway friction coefficients are defined as $\mu_{\text{r,TO}} = 0.02$ and $\mu_{\text{r,L}} = 0.065$ based on a smooth, paved surface [2]. In addition, $\mu_{\text{r,L}} > \mu_{\text{r,TO}}$ since brakes are engaged during the landing procedure. With all of the baseline forces defined, the instantaneous effective forces for the takeoff and landing configurations are obtained with Eq. (12) and Eq. (13), respectively.

$$L_{TO} = C_{L,TO}\frac{1}{2}\,\rho_0 V^2 S \tag{8}$$

$$L_L = C_{L,L}\frac{1}{2}\,\rho_0 V^2 S \tag{9}$$

$$D_{TO} = C_{D,TO}\frac{1}{2}\rho_0 V^2 S \tag{10}$$

$$D_L = C_{D,L}\frac{1}{2}\rho_0 V^2 S \tag{11}$$

$$F_{\text{eff},TO} = T_{\max} - \left[D_{TO} + \mu_{\text{r,TO}}\left(W_{MTOW} - L_{TO}\right)\right] \tag{12}$$

$$F_{\text{eff},L} = -T_{\text{rev}} - \left[D_L + \mu_{\text{r,L}} W_{MTOW}\right] \tag{13}$$

Since the effective forces change with time, the instantaneous acceleration $\ddot{x}\,(t)$ is obtained with Eq. (14), a manipulated expression of the original 1-D equation of motion described by Eq. (1) on pg. 3. Given $\ddot{x}\,(t)$, the instantaneous ground speed $\dot{x}\,(t)$ is numerically approximated with the explicit Euler method as shown in Eq. (15), with a timestep of $dt = 0.1s$ [10]. Since wind conditions are neglected in the baseline study, the instantaneous ground speed is equivalent to the airspeed. Given $\dot{x}\,(t)$, the instantaneous position $x\,(t)$ is approximated with the same explicit Euler method as shown in Eq. (16). Regarding initial conditions, the aircraft is initially at rest and all of the parameters (e.g., ground speed, lifting force, etc.) are initialized to zero. The boundary condition used in the present work is the length of the runway $S_{28\text{R}}$.

$$\ddot{x}\,(t) = \frac{g_0}{W_{MTOW}} F_{\text{eff}} \tag{14}$$

$$\dot{x}\,(t) = \dot{x}\,(t - dt) + \ddot{x}\,(t - dt)\,dt \tag{15}$$

$$x\,(t) = x\,(t - dt) + \dot{x}\,(t - dt)\,dt \tag{16}$$

The numerical scheme described by Eq. (15) above is implemented to obtain two velocity profiles: one for the takeoff configuration and one for the landing configuration. Moreover, the intersection point between the takeoff and landing velocity profiles is determined, and the RTO speed is numerically approximated to be $V_1 = 63.9\ {}^{m}/_{s}$ [11, 12]. To validate the baseline model, the nominal takeoff distance $S_{TO,\text{pub}}$, as well as the nominal landing distance $S_{L,\text{pub}}$ are numerically approximated. Compared to the published A380 data (refer to Table 1 on pg. 4), $S_{TO,\text{pub}}$ and $S_{L,\text{pub}}$ obtained from the numerical scheme (refer to Fig. 2 on the following page) have percent differences of -3.63% and 0.2%, respectively. Given the results in Fig.2, the numerical scheme described in this section is deemed valid and is used to assess the impact of environmental factors on the RTO speed of an A380 at MTOW.

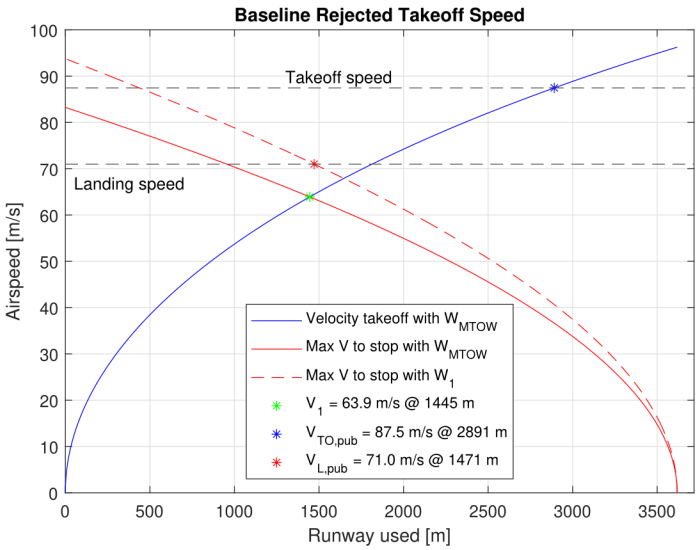

Fig. 2 Baseline RTO speed of an Airbus A380

V. Environmental Factors and Sensitivity Analysis

Environmental factors such as wind speed and unfavorable runway conditions are implemented into the baseline numerical scheme described in Sect. 4 to assess realistic impacts on the RTO speed as well as the location of the RTO speed along the runway. Regarding wind conditions, pure headwinds and tailwinds are included in the model to capture both favorable and unfavorable wind conditions. Regarding surface conditions, the two runway classes selected for this environmental study are dry and wet. The dry runway conditions used in the environmental study are the same conditions used in the baseline study. Moreover, for wet runway conditions it is assumed that the depth of standing water along the runway is less than 3-mm, according to the FAA [9].

A. Environmental Inputs

Realistic headwind and tailwind conditions were obtained from 2022 KSFO METAR observations, which were made weekly for one year, via the ASOS network available through Iowa Environmental Mesonet (IEM) [7]. The maximum headwind and tailwind conditions were approximately 16.5-kts and 3.3-kts, respectively [7]. Moreover, a factor of safety (FoS) of 1.50 is used to account for stronger, unforeseen wind conditions. Once converted to the appropriate units, the design wind speed array used in the environmental model was $-2.55\ {}^{m}/_{s} \leq V_{\text{wind}} \leq 12.70\ {}^{m}/_{s}$. In addition, the wind conditions ultimately impact the aerodynamic forces described in Eqs. (8) through (11), and the new airspeed is obtained with Eq. (17) below. Headwinds are added to the ground speed $\dot{x}$ due to the increase in aerodynamic performance during the ground roll, whereas tailwinds are subtracted from $\dot{x}\,(t)$ and ultimately reduce the lift due to a smaller value of V [3].

$$V = \dot{x}\,(t) \pm V_{\text{wind}} \tag{17}$$

Regarding the dry runway surface conditions, the dimensionless runway friction coefficient values for the takeoff and landing configuration are $\mu_{\text{r,TO}} = 0.02$ and $\mu_{\text{r,L}} = 0.065$, identical to the baseline study. Based on acceptable runway surface expressions for the landing configuration, the friction coefficient for the wet runway is approximated to be $\mu_{\text{r}_{\text{wet}},\text{L}} = 0.5\mu_{\text{r,L}}$ [9]. Moreover, the present work assumes the same factor is applied to the takeoff configuration, and $\mu_{\text{r}_{\text{wet}},\text{TO}} = 0.5\mu_{\text{r,TO}}$. As a result, the design runway friction coefficient arrays for the takeoff and landing configurations are $0.01 \leq \mu_{\text{r,TO}} \leq 0.02$ and $0.033 \leq \mu_{\text{r,L}} \leq 0.065$, respectively.

B. Sensitivity Analysis

The two independent variables used in the 2-D sensitivity analysis were wind speed and runway surface conditions. The overall objective of the present work is to determine how headwinds, tailwinds, and varying runway surface

conditions impact V_1. The environmental model was built on top of the proven baseline model described in Sect. 4. Furthermore, the environmental model calculated the RTO speed for every condition within the design wind speed array, given a pair of runway friction coefficients for the takeoff and landing configurations (e.g., tailwind with a wet runway, headwind with a wet runway, etc.). As a result, the RTO speed of an A380 under various environmental conditions is presented in Fig. 3(a) on the following page.

The independent variables had different impacts on V_1, as well as the location of the RTO speed S_1, for an A380 at MTOW. For example, V_1 increased parabolically as the runway friction coefficient increased. Moreover, the parabolic trend is expected because the runway friction coefficient is impacted by the lifting force, which depends on the square of the airspeed (refer to Eq. (12) and Eq. (13) on pg. 6). Additionally, if the wind speed was held constant, V_1 evaluated under dry runway surface conditions conditions increased by approximately 12.0% when compared to wet runway conditions. Of the independent variables, the wind speed had the largest impact on V_1 (refer to Fig. 3(a) below). With the strongest tailwind and headwind considered, V_1 increased by approximately 20.4% when the runways surface conditions were held constant. Moreover, the linear trend is expected because V_{wind} is added or subtracted from the ground speed (refer to Eq. (17)) on pg. 7) based on the wind conditions.

The location of the RTO speed S_1 is numerically approximated and is shown in Fig. 3(b) below. Regarding S_1, the runway surface conditions have a significant impact compared to the wind speed. Assuming constant wind conditions, S_1 evaluated under dry runway conditions increased by approximately 40% when compared to wet surface conditions. On the other hand, the varying wind speed had little effect on S_1. For example, S_1 increased approximately 3.1% when the maximum tailwind and headwind conditions were considered.

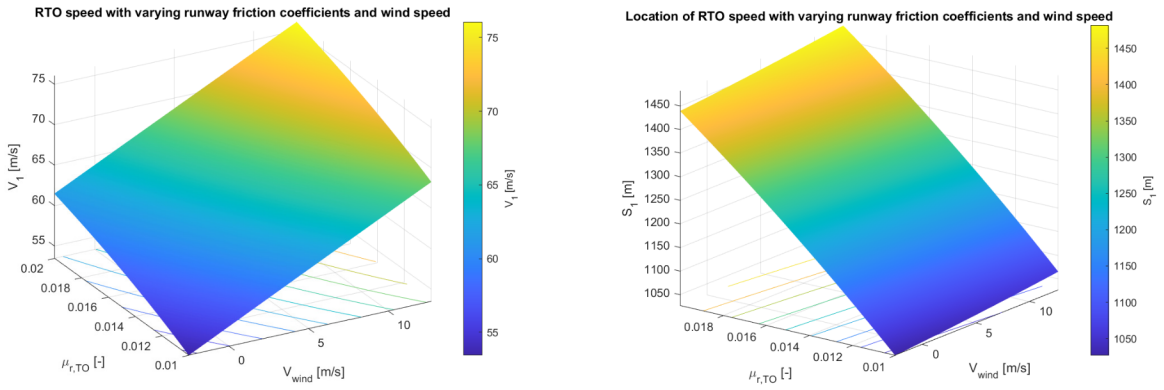

(a) RTO speed

(b) Location of RTO speed along the runway

Fig. 3 Environmental impacts on the RTO speed of an A380

For verification purposes, the landing distance with respect to V_1 is numerically approximated and presented in Fig. 4 on the following page. Because V_1 is the intersection point between the takeoff velocity profile and the landing velocity profile, the sum of the takeoff and landing distances with respect to V_1 is expected to be equal to the length of runway, $S_{28\text{R}}$. The random environmental inputs selected for verification are presented in Table 4 below. Regarding the takeoff and landing velocity profiles with respect to V_1, the length of runway used was numerically calculated to be 1,326.21 m and 2,291.79 m, respectively. Furthermore, the sum of the takeoff and landing distances with respect to V_1 was equal to $S_{28\text{R}}$.

Table 4 Environmental model verification inputs

Parameter	Value	Units
$\mu_{\text{r,TO}}$	0.0163	–
$\mu_{\text{r,L}}$	0.0547	–
V_{wind}	5.486	m/s

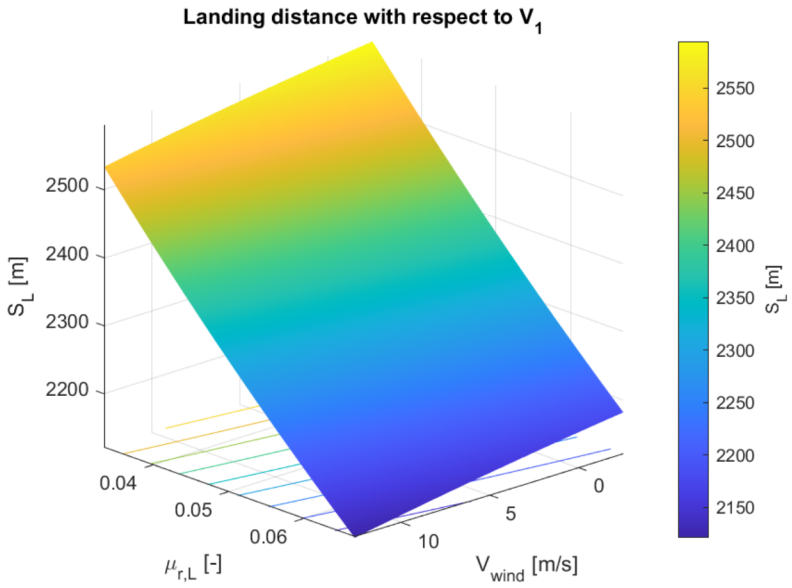

Fig. 4 Landing distance with respect to the RTO speed

VI. Conclusion

The RTO speed of a commercial airliner is a critical parameter that is determined prior to departure to reduce the likelihood of runway excursions in the event of an aborted takeoff. In addition to aircraft specifications, runway dimensions, and intensive thermodynamic properties, environmental factors such as wind speed and runway surface conditions have a significant effect on V_1 and must be considered. In the present work, the environmental model was built on top of the proven baseline case which was validated with published A380 data. The results of the 2-D sensitivity analysis showed the interaction between the varying wind speed and runway surface conditions and the overall impact on V_1 and S_1. Varying wind speed had the largest impact on the value of V_1, whereas runway surface conditions had the largest impact on the location of the RTO point along the runway.

A. Future Work

Several assumptions were made to approximate the RTO speed of an A380 under various environmental conditions. To further refine the accuracy of the model, empirical formulas for various runway surface conditions could be explored. Regarding the effective forces, a sequential 2-step thrust application could be included to capture realistic takeoff procedures. In addition to pure headwinds and tailwinds, a gust model, as well as a crosswind model, could be implemented on top of the constant wind speed to account for drastic environmental changes. In addition, other factors such as multiple engine failures at random locations along the runway could be incorporated into the model.

References

[1] White, W. J., "Takeoff Safety Training Aid," *FAA AC Document No. 120-62*, 1994.

[2] Anderson, J. D., *Introduction to Flight*, 8th ed., McGraw-Hill, New York, 2016, Chap. 6, pp. 522–531.

[3] Zhu, Y., Wang, J., Chen, Y., and Wu, Y., "Calculation of Takeoff and Landing Performance under different Environments," *International Journal of Modern Physics*, Vol. 42, No. 1660174, 2016, pp. 1–12. https://doi.org/10.1142/S2010194516601745.

[4] Xiang, X., Zhang, S., and Xie, L., "Research on Calculation for Rejected Takeoff Distance of Civil Aircraft on Wet and Contaminated Runway," *IPEC*, 2022, pp. 60–63. https://doi.org/10.1145/3544109.3544120.

[5] "Airbus A380 Facts and Figures," *Airbus*, 2021. URL https://www.airbus.com/sites/g/files/jlcbta136/files/2021-12/EN-Airbus-A380-Facts-and-Figures-December-2021_0.pdf.

[6] "Airport Master Record," *FAA Document No. OMB 2120-0015*, 2022.

[7] Herzmann, D. (ed.), *Iowa Environmental Mesonet ASOS Network*, Iowa State University, 2023.

[8] "Aircraft Characteristics - Airport and Maintenance Planning," *Revision No. 17*, 2016. URL https://www.airbus.com/sites/g/files/jlcbta136/files/2021-11/Airbus-Aircraft-AC-A380.pdf.

[9] Jiang, Y., "Review on flight performance certification standard for wet and contaminated runway," *Procedia Engineering*, Vol. 17, Elsevier, 2011, pp. 7–12. https://doi.org/10.1016/j.proeng.2011.10.002.

[10] Lomax, H., Pulliam, T., and Zingg, D., *Fundamentals of Computational Fluid Dynamics*, 1st ed., Springer-Verlag Berlin Heidelberg, New York, 2001, Chap. 6, p. 83. https://doi.org/10.1007/978-3-662-04654-8.

[11] Schwarz, D., "Fast and Robust Curve Intersections," *MATLAB Central File Exchange*, 2023. URL https://www.mathworks.com/matlabcentral/fileexchange/11837-fast-and-robust-curve-intersections.

[12] MATLAB, *version 9.13.0.2105380 (R2022b)*, The MathWorks Inc., Natick, Massachusetts, 2022.